Journal of Sound and Vibration (1997) **200**(4), 401–418

THE EFFECTS OF DYNAMIC ABSORBERS ON THE FORCED VIBRATION OF A CYLINDRICAL SHELL AND ITS COUPLED INTERIOR SOUND FIELD

Y. M. HUANG

Department of Mechanical Engineering, *National Central University*, *Chung-Li*, *Taiwan* 320, *Republic of China*

AND

C. R. FULLER

Department of Mechanical Engineering, *Virginia Polytechnic Institute and State University*, *Blacksburg*, *VA* 24061-0238, *U.S.A.*

(*Received* 3 *October* 1995, *and in final form* 22 *July* 1996)

The vibration and the coupled interior sound field of a closed, elastic cylindrical shell, due to both external point forces and distributed forces, are separately studied in this paper. Multiple dynamic absorbers are then attached to the shell to reduce the vibration and the consequent interior acoustic sound pressure. The dynamic response of the shell and the sound pressure in the interior acoustic cavity, under the influence of absorbers, are obtained using the techniques of substructure synthesis and modal expansion. Analytic solutions are derived. Numerical examples are then studied and discussed. The results show that the addition of dynamic absorbers, if correctly positioned, can successfully reduce the vibration of the shell and the interior acoustic pressure of the sound field enclosed by the shell. Further, the best absorber arrangement is found to be strongly dependent on the type of external forces present. Some general guidelines on absorber design for the reduction of the shell vibration and its interior noise are offered in conclusion. The effects of varying the parameters of the absorbers such as mass, stiffness, and the location of the absorber are also investigated for the two types of external forces.

1. INTRODUCTION

This paper focuses on developing an analytical model for the dynamics of a closed, elastic cylindrical shell with dynamic absorbers and the coupled interior acoustic field. The vibrating shell can serve as a simple model of the fuselage of an aircraft. Two types of general forces, point forces and the distributed pressures, are assumed to exicte the system. Various configurations of absorbers are investigated. The results show that the vibration of the shell and the amplitude of the coupled interior sound pressure can be significantly reduced by adding dynamic absorbers. General discussions on designing techniques of the absorbers for vibration and sound control of the cylindrical shell, for the two types of disturbances, are put forward.

The effects of external forces and sound sources on the vibration of a cylindrical shell and the consequent internal noise have been studied in several publications. Wilby [1] has published a paper which reviews the various methods of predicting the interior sound field of the fuselage due to propellers. The vibration and the enclosed sound field of an infinite cylindrical shell have been investigated by Fuller and Fahy [2] as well as by Fuller [3] by means of wave propagation analysis. Fuller [4] also used this technique to develop a model

0022–460X/97/090401 + 18 $25.00/0/sv960708

of aircraft fuselage dynamics where the synchrophasing effect is included. Thomas *et al*. [5, 6] derived the solutions for the vibration and the enclosed acoustic field of a cylindrical shell with finite length under various forcing conditions.

Many techniques have been developed to reduce the vibration of the cylindrical shell, and the resulting interior noise. Passive control has been the traditional technique used to achieve these goals. In a passive control system, the vibration and the coupled sound are reduced by adding appropriate passive elements or modifying the structure. Neither external energy nor the formulation of control laws are necessary for the use of passive control implementation. There have been achievements in this field especially in reducing the vibration of structures. Berry and Nicolas [7] recently presented a paper, concerning the control of the vibration and the radiated sound of a plate obtained by changing the mass, stiffness, and supporting conditions. General rules were given in their paper for the design of passive control methods for plates. Their conclusions, nevertheless, cannot be applied to the cylindrical shell problem directly due to the significant difference in the dynamic behaviors of the cylindrical shell and the plate. Fuller has also studied the reduction of the interior sound field by changing the parameters of the cylindrical shell [8] or by adding detuned, passive dynamic absorbers [9]. With the exception of these papers, there exists little literature related to the passive vibration and noise control of a cylindrical shell or a fuselage.

Active control methods have become increasingly popular with the recent developments in digital signal processing (DSP) techniques. With fast-calculating computer hardware, real-time control of vibration and noise is becoming practical. Active control techniques have been used to reduce the vibration of structures as well as their resultant noise. Active noise control (ANC) employs microphone error sensors and active acoustic sources to reduce the acoustic pressure in the sound field. Active vibration control (AVC) uses structural error sensors and active vibration inputs to reduce structural vibrations. The use of AVC does not necessarily ensure sound reduction. In fact, the use of AVC to reduce the vibration will often increase the sound radiation. In this case active structural acoustic control (ASAC), in which vibration inputs are employed in conjunction with sound error sensors, is used. Much work related to these methods for the cylindrical shell and the practical analogue of aircraft interior noise have already been presented. Theoretical formulations of AVC for controlling the shell vibration can be found in the work of Jones and Fuller [10], and Brevart and Fuller [11]. Experimental verifications were also conducted by Mandic and Jones [12], Simpson *et al*. [13], and Mathur and Tran [14]. Nelson and Elliott [15] have studied the use of ANC. Thomas, and Bullmore *et al*. have studied the use of AVC and ASAC [5, 6, 16]; while Fuller and his colleague have done much of the theoretical and experimental work on applying ASAC to laboratory and real aircraft fuselages [8, 10, 11, 17].

Though active control methods are effective and give satisfactory results, passive control remains an important vibration and noise control tool. Passive control, compared to the active control, exhibits the advantages of easy implementation, low cost, and no need for external energy. Most importantly, passive control methods never drive the system to instability while the active methods might. Vibration and noise control achieved through the use of dynamic absorbers is the specific passive control method considered in this paper. The techniques for the implementation of absorbers on a simple one- or two-degrees-of-freedom dynamic system are well known [18, 19]. The general rules of absorber design for simple dynamic systems, however, cannot be applied to more complicated structures, such as a shell, because of the existence of relatively high modal density of these structures. In spite of the lack of theoretical derivations, tuned dynamic absorbers have been experimentally implemented to reduce the vibration and the

accompanying noise in real fuselages [20, 21]. The results show that the prospects of successfully using dynamic absorbers for vibration and noise control are good.

2. VIBRATION OF THE CYLINDRICAL SHELL

2.1. EQUATIONS OF MOTION

In this paper a closed, thin circular cylindrical shell with shear diaphragms at both ends as shown in Figure 1 will be considered. The mean radius, the length, and the thickness of the shell are denoted as R, L, and h, respectively. The three independent spatial co-ordinates are chosen to be the axial co-ordinate x, the circumferential co-ordinate θ, and the radial (transverse) co-ordinate r. The corresponding midsurface displacements of the shell are $u_x(x, \theta, t)$, $u_\theta(x, \theta, t)$ and $u_r(x, \theta, t)$ with t representing the time. The matrix equation of motion of the shell vibration, based on the Donnell-Mushtari shell theory [22], can then be obtained as

$$[\mathbf{L}]\{\mathbf{u}\} = \{\mathbf{Q}\}, \tag{1}$$

where $\{\mathbf{u}\} = \{u_x, u_\theta, u_r\}^{\mathrm{T}}$ represents the displacement vector, and $\{\mathbf{Q}\} = \{Q_x, Q_\theta, Q_r\}^{\mathrm{T}}$ is the normalized force vector whose elements are related to the real external forces, f_x, f_θ, and f_r, by

$$Q_x = -f_x/Q, \qquad Q_\theta = -f_\theta/Q, \qquad Q_r = f_r/Q, \tag{2}$$

with $Q = Eh/(1 - \nu^2)R^2$. The symmetric, 3×3, differential matrix operator is defined as

$$[\mathbf{L}] = \begin{bmatrix} R^2\dfrac{\partial^2}{\partial x^2} + \dfrac{1}{2}\dfrac{\partial^2}{\partial\theta^2} - \dot{\rho}\dfrac{(1-\nu^2)R^2}{E}\dfrac{\partial^2}{\partial t^2} & \dfrac{(1+\nu)R}{2}\dfrac{\partial^2}{\partial x\,\partial\theta} & \nu R\dfrac{\partial}{\partial x} \\ \dfrac{(1+\nu)R}{2}\dfrac{\partial^2}{\partial x\,\partial\theta t} & \dfrac{(1+\nu)R^2}{2}\dfrac{\partial^2}{\partial x^2} + \dfrac{\partial^2}{\partial\theta^2} - \rho\dfrac{(1-\nu^2)R^2}{E}\dfrac{\partial^2}{\partial t^2} & \dfrac{\partial}{\partial\theta} \\ \nu R\dfrac{\partial}{\partial x} & \dfrac{\partial}{\partial\theta} & 1 + \hat{h}\nabla^4 + \rho\dfrac{(1-\nu^2)R^2}{E}\dfrac{\partial^2}{\partial t^2} \end{bmatrix} \tag{3}$$

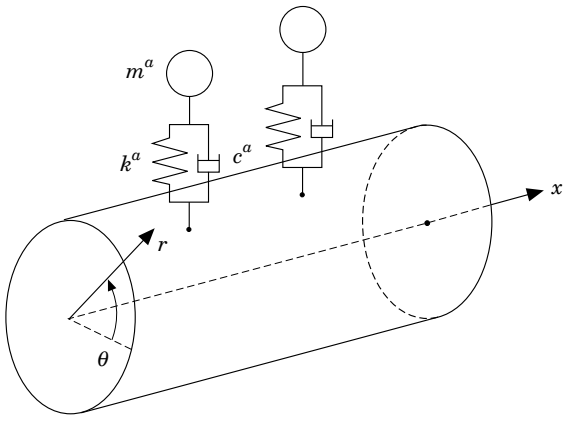

Figure 1. The cylindrical shell and the dynamic absorbers.

where ρ, E, and v are, respectively, the density, the Young's modulus, and the Poisson's ratio of the shell material, $\hat{h} = h^2/12R^2$ is the dimensionless thickness parameter, and $\mathbf{\nabla}^4 = \mathbf{\nabla}^2\mathbf{\nabla}^2 = [R^2(\partial^2/\partial x^2) + (\partial^2/\partial\theta^2)]^2$.

2.2. FREE VIBRATION

The general solution to the free vibration of equation. (1) is of the form

$$\{\mathbf{u}\} = \begin{Bmatrix} A_1 \cos(m_1\pi x/L)\cos(m_2\theta) \\ B_1 \sin(m_1\pi x/L)\sin(m_2\theta) \\ C_1 \sin(m_1\pi x/L)\cos(m_2\theta) \end{Bmatrix} e^{-i\omega t}, \tag{4}$$

or

$$\{\mathbf{u}\} = \begin{Bmatrix} -A_2 \cos(m_1\pi x/L)\sin(m_2\theta) \\ B_2 \sin(m_1\pi x/L)\cos(m_2\theta) \\ -C_2 \sin(m_1\pi x/L)\sin(m_2\theta) \end{Bmatrix} e^{-i\omega t}. \tag{5}$$

Here, ω is the natural frequency of the shell and $m_1\pi/L (m_1 = 1, 2, \ldots.)$ and m_2 ($m_2 = 0, 1, 2, \ldots$) are wave numbers in the x and θ directions, respectively, for matching the boundary conditions at both ends [22]. The constants A_1, B_1, C_1, A_2, B_2, and C_2 are undetermined modal constants and are different for each mode.

The natural frequencies of the cylindrical shell and the corresponding mode shapes can be obtained by substituting the modes (4) and (5) into equation (1). For the detailed calculation of the natural frequencies and modes the reader can refer to the text of Leissa [22]. Three natural frequencies and three sets of mode shapes, with different modal constants, are found to be associated with each combination of (m_1, m_2). Among them, the set of mode shapes with the lowest natural frequency is usually the transverse-vibration dominant mode and is coupled strongly with the enclosed sound field. For simplification, only the displacement in the radial direction, u_r, corresponding to the transverse modes, is considered here for calculating the shell vibration and its associated interior sound pressure.

2.3. FORCED VIBRATION

The radial displacement of the shell, subject to an arbitrary external excitation, can be described as a linear combination of modes, i.e.,

$$u_r(x, \theta, t) = \sum_{m_1=1}^{\infty} \sum_{m_2=0}^{\infty} \sum_{m_3=1}^{2} u_{m_1m_2m_3}(t)\phi_{m_1m_2m_3}(x, \theta), \tag{6}$$

in which the mode shape is written as

$$\phi_{m_1m_2m_3} = \sin(m_1\pi x/L)\cos(m_2\theta + (m_3 - 1)\pi/2) \tag{7}$$

and $u_{m_1m_2m_3}(t)$ represents the modal co-ordinate corresponding to the vibration mode (m_1, m_2, m_3). In the above expression, $m_3 = 1$ associates with the so-called symmetric response with respect to co-ordinate θ and $m_3 = 2$ associates with the anti-symmetric response.

The modal equation can then be derived, using the orthogonal properties of the mode shapes, in the form of

$$\ddot{u}_{m_1m_2m_3} + 2\zeta\omega_{m_1m_2}\dot{u}_{m_1m_2m_3} + \omega^2_{m_1m_2}u_{m_1m_2m_3} = q_{m_1m_2m_3}(t)/M_{m_1m_2}, \tag{8}$$

where $m_1 = 1, 2, \ldots,$ $m_2 = 0, 1, 2, \ldots,$ $m_3 = 1, 2,$ the dot notation represents the derivative with respect to the time t, and $q_{m_1m_2m_3}(t)$ is the modal force that will be discussed later. The notation $\omega_{m_1m_2}$ denotes the radial or transverse natural frequency of mode (m_1, m_2). The modal mass $M_{m_1m_2} = \rho(1-\mu^2)(1 - A_1^2 - B_1^2)/E$, on the right side of the modal equation, is a function of the shell parameters as well as the modal constants. An additional modal damping term is introduced to each modal equation in which ζ represents the modal damping ratio and is taken to be the same for each vibration mode.

Two different types of external forces, acting in the radial direction, are separately considered in this work. (1) Point forces are first used to excite the motion of the cylindrical shell. Each point force is expressed as

$$f_r(x, \theta, t) = F^1 \, \delta_2(x - \bar{x}, \theta - \bar{\theta}) \, \mathrm{e}^{-\mathrm{i}\Omega t} \tag{9}$$

and is applied to the shell at the location $(x = \bar{x}, \theta = \bar{\theta})$. The notation F^1 represents the complex magnitude of the force, Ω represents the excitation frequency, and δ_2 is the two-dimensional Dirac delta function. This type of force is the representation of the structural inputs due to engine out-of-balance forces. (2) Uniformly distributed pressures are chosen as the second type external excitation. Every distribution can then be represented in the form of

$$\begin{aligned} f_r(x, \theta, t) = F^2[&U(x - (\bar{x} - a/2)) - U(x - (\bar{x} + a/2))] \\ &\times [U(\theta - (\bar{\theta} - b/2R)) - U(\theta - (\bar{\theta} + b/2R))] \, \mathrm{e}^{-\mathrm{i}\Omega t}. \end{aligned} \tag{10}$$

In this expression, U represents the step function, $(x = \bar{x}, \theta = \bar{\theta})$ is the center of the distributed pressure (called center location in brief) with width a in the axial direction and b in the radial direction, and F^2 is the complex magnitude of the pressure. This pressure distribution is an idealized mathematical model of the external pressure on the fuselage due to an engine.

Suppose that these two types of external forces are individually applied to the shell in the radial direction. The modal force to the shell becomes

$$q_{m_1m_2m_3}(t) = \int_0^{2\pi} \int_0^L \frac{f_r(x, \theta, t)}{Q} \, \phi_{m_1m_2m_3}(x, \theta) \, \mathrm{d}x \, \mathrm{d}\theta. \tag{11}$$

The radial displacement can then be obtained from equation (6) after all the modal equations (8) are solved. The displacement can also be rewritten as

$$u_r(x, \theta, t) = \sum_k H^\ell(x, \theta, \bar{x}_k, \bar{\theta}_k, \Omega) F_k^\ell \, \mathrm{e}^{-\mathrm{i}\Omega t}, \tag{12}$$

where $H^\ell(x, \theta, \bar{x}_k, \bar{\theta}_k, \Omega)$ is the frequency response function at shell location (x, θ) subject to one external force of the ℓth type acting at $(\bar{x}_k, \bar{\theta}_k)$, and Σ_k sums the responses due to all the external forcing functions.

The kinetic energy (KE) of the shell, for evaluation of the overall vibration of the shell, is defined as

$$KE = \tfrac{1}{2} \int_V \rho \dot{u}_r \dot{u}_r^* \, \mathrm{d}V = \tfrac{1}{2} \rho h R \Omega^2 \sum_{m_1=1}^{\infty} \sum_{m_2=0}^{\infty} \sum_{m_3=1}^{2} U_{m_1m_2m_3} U^*_{m_1m_2m_3} \Delta_{m_1m_2m_3}, \tag{13}$$

where the notation * denotes the complex conjugate of a complex variable, V is the total

volume of the shell material, and $\Delta_{m_1m_2m_3} = h\int_0^{2\pi}\int_0^L \phi^2_{m_1m_2m_3}\,\mathrm{d}x\,\mathrm{d}\theta$. Here, $U_{m_1m_2m_3}$ represents complex amplitude of the corresponding modal co-ordinate and $u_{m_1m_2m_3}(t) = U_{m_1m_2m_3}\,\mathrm{e}^{-\mathrm{i}\Omega t}$.

3. FORMULATION OF DYNAMIC ABSORBERS

Suppose that M absorbers, located at (x_j, θ_j), $j = 1, 2, \ldots, M$, are connected to the shell in the radial direction as illustrated in Figure 1. The mean, the stiffness, and the damping ratio of each absorber are represented by m_j^a, k_j^a, and ζ_j^a, respectively. The variable $\omega_j^a = \sqrt{k_j^a/m_j^a}$ is usually called the natural of the jth absorber while $c_j^a = 2\zeta_j^a\sqrt{m_j^a k_j^a}$ denotes the damping coefficient of the jth absorber. The equations of motion for the jth absorber are

$$m_j^a\ddot{d}_j = -f_j^a, \qquad f_j^a = k_j^a(d_j - u_{rj}) + c_j^a(\dot{d}_j - \dot{u}_{rj}), \tag{14, 15}$$

in which $d_j(t) = D_j\,\mathrm{e}^{-\mathrm{i}\Omega t}$ is the radial displacement of the absorber, and $f_j^a(t) = F_j^a\,\mathrm{e}^{-\mathrm{i}\Omega t}$ denotes the resultant point force caused by the jth absorber acting on the shell. In equation (15), $u_{rj}(t)$ is the radial displacement of the shell at (x_j, θ_j), and is a result of the combined effects of all the external forces and the forces from the absorbers, that is,

$$u_{rj} = U_{rj}\,\mathrm{e}^{-\mathrm{i}\Omega t} = \sum_k H_{kj}^{\ell}F_k^{\ell}\,\mathrm{e}^{-\mathrm{i}\Omega t} + \sum_{s=1}^{M} H_{sj}^a F_s^a\,\mathrm{e}^{-\mathrm{i}\Omega t}. \tag{16}$$

Here, $H_{kj}^{\ell} = H^{\ell}(x_j, \theta_j, \bar{x}_k, \bar{\theta}_k, \Omega)$ represents the frequency response function at (x_j, θ_j) due to the ℓth type external force located at $(\bar{x}_k, \bar{\theta}_k)$, and $H_{sj}^a = H^1(x_j, \theta_j, x_s, \theta_s, \Omega)$ is the frequency response function at (x_j, θ_j) generated by the point force $f_s^a(t)$ from the sth absorber. Combining equations (14), (15) and (16) yields the matrix equation

$$\left[\begin{array}{cccc|cccc}
1-\hat{k}_1^a & 0 & \cdots & 0 & \hat{k}_1^a & 0 & \cdots & 0 \\
0 & 1-\hat{k}_2^a & \cdots & 0 & 0 & \hat{k}_2^a & \cdots & 0 \\
\vdots & \vdots & \ddots & \vdots & \vdots & & \ddots & \vdots \\
0 & 0 & \cdots & 1-\hat{k}_M^a & 0 & 0 & \cdots & \hat{k}_M^a \\
\hline
-\Omega^2 m_1^a H_{11}^a & -\Omega^2 m_2^a H_{21}^a & \cdots & -\Omega^2 m_M^a H_{M1}^a & 1 & 0 & \cdots & 0 \\
-\Omega^2 m_1^a H_{12}^a & -\Omega^2 m_2^a H_{22}^a & \cdots & -\Omega^2 m_M^a H_{M2}^a & 0 & 1 & \cdots & 0 \\
\vdots & \vdots & \ddots & \vdots & \vdots & \vdots & \ddots & \vdots \\
-\Omega^2 m_1^a H_{1M}^a & -\Omega^2 m_2^a H_{2M}^a & \cdots & -\Omega^2 m_1^a H_{MM}^a & 0 & 0 & \cdots & 1
\end{array}\right]
\left\{\begin{array}{c} D_1 \\ D_2 \\ \vdots \\ D_M \\ \hline U_{r1} \\ U_{r2} \\ \vdots \\ U_{rM} \end{array}\right\}$$

$$= \left\{0, 0, \ldots, 0, \sum_k H_{k1}^{\ell}F_k^{\ell}, \sum_k H_{k2}^{\ell}F_k^{\ell}, \ldots, \sum_k H_{kM}^{\ell}F_k^{\ell}\right\}^{\mathrm{T}}, \tag{17}$$

where $\hat{k}_j^a = (k_j^a - \mathrm{i}\Omega c_j^a)/(\Omega^2 m_j^a)$, $j = 1, 2, \ldots, M$. This is an algebraic, matrix equation of $2M$ linear equations. The complex amplitudes of absorbers' displacements D_j, $j = 1, 2, \ldots, M$, and as a consequence, the force amplitudes F_j^a of the absorbers can be easily obtained.

The radial displacement of the absorber-connected shell, subject to the external forces,

can then be expressed as

$$u_r(x, \theta, t) = \left[\sum_k H^{\prime}(x, \theta, \bar{x}_k, \bar{\theta}_k, \Omega) F_k^{\prime} + \sum_{j=1}^{M} H^{1}(x, \theta, x_j, \theta_j, \Omega) F_j^{a} \right] \mathrm{e}^{-\mathrm{i}\Omega t}. \tag{18}$$

The sound field inside the cylindrical shell will be calculated based on the above expansion form of the radial displacement.

4. INTERIOR SOUND FIELD

4.1. WAVE EQUATION

The interior sound field of the cylindrical shell is governed by the wave equation [23]

$$\nabla^2 p - (1/\tilde{c}^2)\partial^2 p/\partial t^2 = -\tilde{\rho}\partial s/\partial t \tag{19}$$

in which

$$\nabla = \frac{1}{4}\frac{\partial}{\partial r}\left(r\frac{\partial p}{\partial r}\right) + \frac{1}{r^2}\frac{\partial^2}{\partial \theta^2} + \frac{\partial^2}{\partial x^2},$$

$\tilde{c}$ denotes the propagating velocity of the sound wave in air, $\tilde{\rho}$ is the density of the air, and $s(x, \theta, r, t)$ denotes the volume velocity per unit volume of a sound source in the acoustic field. If the boundary conditions of the sound field are assumed to be rigid boundaries, the natural frequency of the (n_1, n_2, n_3) acoustic mode can be represented as [24]

$$\tilde{\omega}_{n_1 n_2 n_3} = \tilde{c}\sqrt{(n_1\pi/L)^2 + \kappa_{n_2 n_3}^2}, \tag{20}$$

where $n_1 = 0, 1, \ldots$, $n_2 = 0, 1, \ldots$, and $n_3 = 1, 2, \ldots$. The radial acoustic wave number is represented by $\kappa_{n_2 n_3}$, and $\kappa_{n_2 n_3} R$ is the n_3th zero of the derivative of the first kind Bessel's function J_{n_2} of order n_2. There are two mode shapes,

$$\psi_{n_1 n_2 n_3 n_4}(x, \theta, r) = \cos(n_1\pi x/L)\cos(n_2\theta + (n_4 - 1)\pi/2)\mathrm{J}_{n_2}(\kappa_{n_2 n_3} r), \tag{21}$$

with $n_4 = 1$ for the symmetric mode or $n_4 = 2$ for the anti-symmetric mode, associated with each natural frequency $\tilde{\omega}_{n_1 n_2 n_3}$.

4.2. SOUND PRESSURE DUE TO VIBRATION OF THE SHELL

The sound pressure induced by any sound source in the acoustic field has the eigenfunction expansion form

$$p(x, \theta, r, t) = \sum_{n_1=0}^{\infty}\sum_{n_2=0}^{\infty}\sum_{n_3=1}^{\infty}\sum_{n_4=1}^{2} p_{n_1 n_2 n_3 n_4}(t)\psi_{n_1 n_2 n_3 n_4}(x, \theta, r). \tag{22}$$

In the above summation, each modal pressure $p_{n_1 n_2 n_3 n_4}(t)$ of the acoustic system is obtained by solving the acoustic modal equation [23]

$$\ddot{p}_{n_1 n_2 n_3 n_4} + 2\tilde{\zeta}\tilde{\omega}_{n_1 n_2 n_3}\dot{p}_{n_1 n_2 n_3 n_4} + \tilde{\omega}_{n_1 n_2 n_3}^2 p_{n_1 n_2 n_3 n_4}$$

$$= -\frac{\tilde{\rho}\tilde{c}^2}{\Delta_{n_1 n_2 n_3 n_4}}\int_0^R\int_0^{2\pi}\int_0^L r\dot{s}(x, \theta, r, t)\psi_{n_1 n_2 n_3 n_4}(x, \theta, r)\,\mathrm{d}x\,\mathrm{d}\theta\,\mathrm{d}r, \tag{23}$$

wherein $\Delta_{n_1n_2n_3n_4} = \int_0^R \int_0^{2\pi} \int_0^L r\psi^2_{n_1n_2n_3n_4}(x, \theta, r)\,\mathrm{d}x\,\mathrm{d}\theta\,\mathrm{d}r$. The acoustic attenuation effect of the air is represnted by an additional acoustic modal damping ratio $\tilde{\zeta}$ in each modal equation of equation (23).

The vibration of the cylindrical shell in the radial direction can create high levels of noise in its interior sound field. In order to calculate the sound pressure due to the vibrating shell, the structure, i.e., the boundary of the sound field, is first treated as the rigid wall. Next, the vibrating boundary is represented as a distributed sound source for the acoustic system [23]. Note that in the calculation the force on the structure due to interior acoustic pressure is not considered. This is because the external force on the shell is much larger than the force from the interior pressure. The influence on the shell dynamics and on the acoustic field due to the interior sound inside the shell is usually neglected [3–6, 16]. Besides the great difference in magnitudes of these two types of forces, solving the fully coupled structural-acoustic system requires a great effort. To include the interior pressure in the calculation of the shell dynamics only complicates the solving procedure but gains no better accuracy of the results. Therefore, the resultant shell vibration as well as the associate interior acoustic field, obtained by the method described above, will approach the fully coupled solutions even though the boundary conditions of the sound field are not exactly satisfied and the effects of the interior pressure are neglected.

To obtain the sound pressure inside the cylindrical shell, an infinitesimal area of the moving shell is considered as an elemental source. This small piece of shell, located at $(\hat{x}, \hat{\theta})$ and with area $R\,\mathrm{d}\hat{x}\,\mathrm{d}\hat{\theta}$, is a sound source of the sound field with a strength given by

$$s = -\dot{u}_r(\hat{x}, \hat{\theta}, t)R\,\mathrm{d}\hat{x}\,\mathrm{d}\hat{\theta}\delta_3(x - \hat{x}, \theta - \hat{\theta}, r - R), \tag{24}$$

where $\dot{u}_r(\hat{x}, \hat{\theta})$ is the radial vibrating velocity of the shell at the source location $(\hat{x}, \hat{\theta})$ and δ_3 is the three-dimensional Dirac-delta function.

The wave equation (19) then becomes

$$\nabla^2 p - (1/\tilde{c}^2)\partial^2 p/\partial t^2 = -\tilde{\rho}\Omega^2 u_r(\hat{x}, \hat{\theta})R\,\mathrm{d}\hat{x}\,\mathrm{d}\hat{\theta}\delta_3(x - \hat{x}, \theta - \hat{\theta}, r - R), \tag{25}$$

with u_r given in equation (6) or equation (18), and Ω is the vibrating frequency of the shell. The modal equation for the acoustic system can be rewritten as

$$\ddot{p}_{n_1n_2n_3n_4} + 2\tilde{\zeta}\tilde{\omega}_{n_1n_2n_3}\dot{p}_{n_1n_2n_3n_4} + \tilde{\omega}^2_{n_1n_2n_3}p_{n_1n_2n_3n_4}$$

$$= -\frac{\tilde{\rho}\tilde{c}^2\Omega^2}{\Delta_{n_1n_2n_3n_4}} \sum_{m_1=1}^{\infty} \sum_{m_2=0}^{\infty} \sum_{m_3=1}^{2} U_{m_1m_2m_3}\phi_{m_1m_2m_3}(\hat{x},\hat{\theta})\psi_{n_1n_2n_3n_4}(\hat{x}, \hat{\theta}, R)R\,\mathrm{d}\hat{x}\,\mathrm{d}\hat{\theta}\,\mathrm{e}^{-\mathrm{i}\Omega t}. \tag{26}$$

In order to obtain the effects from the entire vibrating shell, equation (26) is integrated over the entire shell surface. The interior modal pressure is then given by

$$\ddot{p}_{n_1n_2n_3n_4} + 2\zeta_a\tilde{\omega}_{n_1n_2n_3}\dot{p}_{n_1n_2n_3n_4} + \tilde{\omega}^2_{n_1n_2n_3}p_{n_1n_2n_3n_4}$$

$$= -\frac{\tilde{\rho}\tilde{c}^2\Omega^2 R}{\Delta_{n_1n_2n_3n_4}}\mathrm{e}^{\mathrm{i}\Omega t} \sum_{m_1=1}^{\infty} \sum_{m_2=0}^{\infty} \sum_{m_3=1}^{2} U_{m_1m_2m_3}C. \tag{27}$$

The constant $C = C(m_1, m_2, m_3, n_1, n_2, n_3, n_4)$ is defined in the integration form

$$C = \int_0^L \int_0^{2\pi} \phi_{m_1m_2m_3}(\hat{x}, \hat{\theta})\psi_{n_1n_2n_3n_4}(\hat{x}, \hat{\theta}, R)\,\mathrm{d}\hat{x}\,\mathrm{d}\hat{\theta}. \tag{28}$$

TABLE 1

System parameters

	System parameter	Value
Shell	L (m)	16·0
	R (m)	1·3
	h (m)	0·0012
	E (N/m^2)	$7{\cdot}1 \times 10^{10}$
	v	0·31
	ρ (kg/m^3)	2700·0
	ζ	0·3
Air	$\tilde{c}$ (m/sec)	343·0
	$\tilde{\rho}$ (kg/m^3)	1·21
	$\tilde{\zeta}$	0·05
Excitation	Location	
		$(0{\cdot}35L, -5^\circ)$
		$(0{\cdot}35L, 185^\circ)$
	Ω (Hz)	88

A similar expression representing the sound pressure was also obtained by Thomas *et al*. [6]. Due to the symmetry of the cylindrical shell and the interior sound field, the coupling of vibration modes and acoustic modes is quite selective [6, 8]. The non-zero constant C exists only when $m_1 - n_1$ is an odd number, $m_2 = n_2$, and $m_3 = n_4$. Provided that the response of the vibrating shell has been obtained, the sound pressure distribution in the shell can be determined by solving the acoustic modal equations (27) and by the summation of all the modal pressures $p_{n_1n_2n_3n_4}$ as given in equation (22).

The best indication of the overall noise in a sound field is the potential energy (PE) within the field which is defined for the given volume of the acoustic field $\tilde{V}$ as

$$PE = \frac{1}{2\tilde{\rho}\tilde{c}^2}\int_{\tilde{V}} p(x, \theta, r, t)p^*(x, \theta, r, t)\,\mathrm{d}V$$

$$= \frac{1}{2\tilde{\rho}\tilde{c}^2}\sum_{n_1=0}^{\infty}\sum_{n_2=0}^{\infty}\sum_{n_3=1}^{\infty}\sum_{n_4=1}^{2} P_{n_1n_2n_3n_4}P^*_{n_1n_2n_3n_4}\Delta_{n_1n_2n_3n_4}, \tag{29}$$

in which $P_{n_1n_2n_3n_4}$ is the complex amplitude of the modal pressure, i.e., $p_{n_1n_2n_3n_4}(t) = P_{n_1n_2n_3n_4}\,\mathrm{e}^{-\mathrm{i}\Omega t}$.

5. NUMERICAL RESULTS AND DISCUSSIONS

The geometry of the cylindrical shell and the material properties used here (listed in Table 1) were originally chosen by Thomas *et al*. [5, 6] based on a consideration of the characteristics of a B.Ae 748 test aircraft. However, the values of the thickness h and the modal damping ratio ζ of the shell were selected so as to match the measured accelerations of the aircraft fuselage instead of their actual values [16].

5.1. NATURAL FREQUENCIES

The *in-vacuo* natural frequencies (Hz) of the transverse modes of the vibrating shell are given in Figure 2. The natural frequencies are found to increase as m_1 increases. They

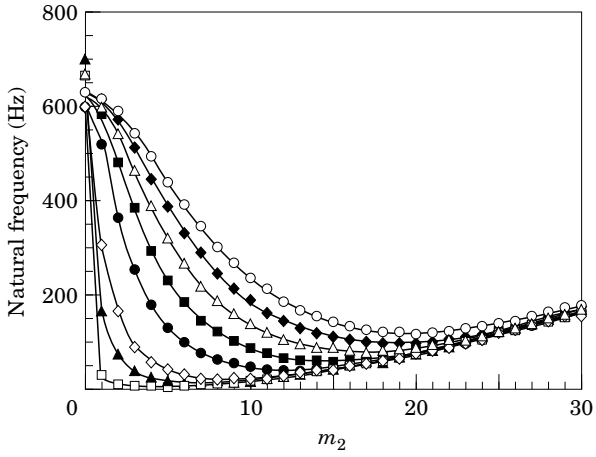

Figure 2. Natural frequencies of the cylindrical shell: m_1 values: —□—, 1; —▲—, 3; —◇—, 5; —●—, 10; —■—, 15; —△—, 20; —◆—, 25; —○—, 30.

decrease, as m_2 becomes larger, and then increase again at a very slow rate after a specific value of m_2. The slowly increasing property of the natural frequencies is mainly due to the small thickness of the shell chosen here. A detailed discussion of this property can be found in Leissa's book [24]. Hence, numerous natural modes exist while the excitation frequency of the external force is greater than 80 Hz. The presence of the relatively high modal density in the shell suggests that many terms will be needed in the modal expansion of the vibration if the excitation frequency Ω is at or above this frequency value.

Figures 3(a) and (b) show the natural frequencies of the acoustic field with rigid boundaries for $n_3 = 1$ and $n_3 = 2$, respectively. The acoustic natural frequencies are close to each other while n_1 is small and their values increase with n_1. From the figures, one can also see that these frequencies rapidly increase with increasing n_2 and n_3. No sign of the high modal density, which exists in the vibration of the shell, is found in the acoustic system within the lower frequency range.

The acoustic energy efficiencies $\alpha_{m_1 m_2}$, of the different vibration modes are illustrated in Figure 4. The energy efficiency, $\alpha_{m_1 m_2}$, is defined as the resultant acoustic potential energy

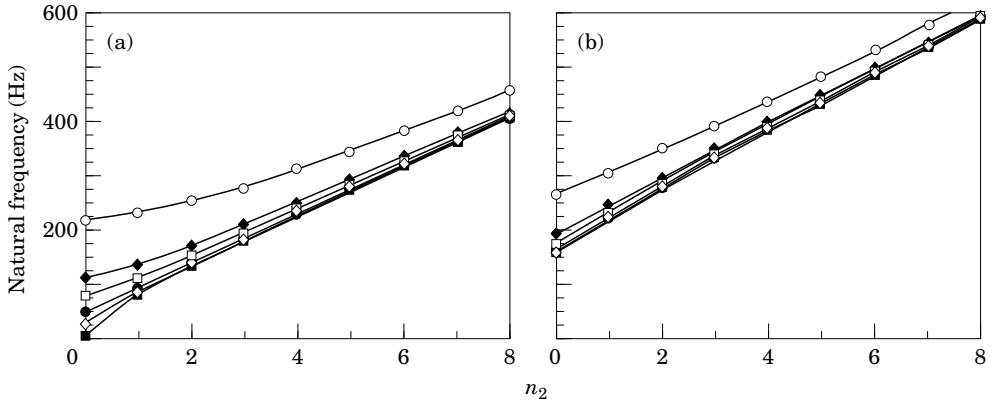

Figure 3. Natural frequencies of the sound field. (a) $n_3 = 1$, (b) $n_3 = 2$: n_1 values: —■—, 1; —◇—, 2; —●—, 4; —□—, 7; —◆—, 10; —○—, 20.

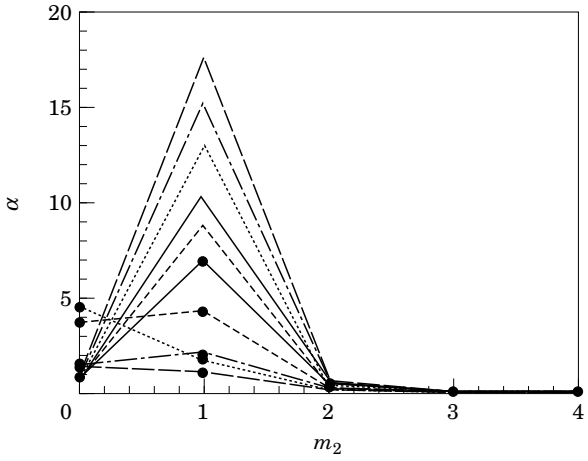

Figure 4. Energy efficiencies of different vibrating modes. m_1 values: ——, 1; – – –, 2; –.–.–., 3; . . . . . , 4; — — —, 5; ——●——, 6; – –●– –, 7; .–.–●–.–., 8; . . . .●. . . , 9; — —●— —, 10.

when there is only the (m_1, m_2) vibration mode of unit kinetic energy excited. Note that the energy efficiencies are highly dependent on the excitation frequency Ω and that this figure only shows the coefficients for the case of $\Omega = 88$ Hz. The vibrating modes of $m_2 = 1$ seem to have the most significant effect on the internal acoustic field. This is due to the fact that the natural frequencies of the (4, 1, 1) and (3, 1, 1) acoustic modes are quite close to the excitation frequency $\Omega = 88$ Hz, and therefore are easily excited by the external forces or the sound sources at that frequency. The vibration modes with $m_2 = 1$, from the calculation of the constant C, are found to give the greatest contribution to these two acoustic modes. From the figure, we can observe that several vibrating modes with $m_2 = 0$ and corresponding to the acoustic mode (8, 0, 1), which has a natural frequency close to the excitation frequency 88 Hz, are also important to the acoustic field. Thus, as discussed in the previous work by Fuller [4], Figure 4 implies that only selected structural modes will couple well with their interior acoustic field.

5.2. RESULTS DUE TO EXTERNAL POINT FORCES

The effects of using dynamic absorbers to reduce the vibration of the shell, subject to point forces, and the resultant sound pressure in the enclosed acoustic cavity are first investigated. Consider two point forces, in the radial direction, applied to the cylindrical shell at $\bar{x} = 0{\cdot}35L$, $\bar{\theta} = -5^\circ$, and 185°. These two external forces used here are assumed to have the same excitation frequency as well as a fixed phase difference. The phase angle θ_p defined in this paper is the phase lead of the force at $(0{\cdot}35L, 185^\circ)$ relative to the force at $(0{\cdot}35L, -5^\circ)$ and is referred to as the synchrophase angle [4]. Unless mentioned otherwise, the natural frequencies of all absorbers are selected with the same value as the excitation frequency, i.e., tuned dynamic absorbers are assumed, and the damping ratios of the absorbers are set to be 0·02. Table 2 gives the change in the kinetic energy (ΔKE) of the vibration and the change in the potential energy (ΔPE) of the total sound pressure in the acoustic field for various implementations of dynamic absorbers and various force parameters. At first, these two external forces are assumed to be in phase ($\theta_p = 0^\circ$). In case 1.1, only one absorber placed at the point $(0{\cdot}35L, -5^\circ)$ is used and its mass is chosen to be 40 kg which is about 1/10 of the mass of the cylindrical shell. Since the two external

TABLE 2

Reduction in KE and PE for external point forces

Case	Δ *KE* (dB)	Δ *PE* (dB)	θ_p(°)	locations of absorbers		m^a
1·1	−1·42	14·66	0	(0·35*L*, −5°)		40 kg × 1
1·2	−61·79	−61·79	0	(0·35*L*, −5°)	(0·35*L*, 185°)	20 kg × 2
1·3	−61·80	−62·69	0	(0·35*L*, −5°)	(0·35*L*, 185°)	20 kg × 2
				(0·35*L*, 90°)	(0·35*L*, 270°)	10 kg × 2
1·4	−61·56	−68·57	0	(0·35*L*, −5°)	(0·35*L*, 185°)	20 kg × 2
				(0·32*L*, −5°)	(0·32*L*, 185°)	10 kg × 4
				(0·38*L*, −5°)	(0·38*L*, 185°)	
1·5	−61·61	−68·48	0	(0·35*L*, −5°)	(0·35*L*, 185°)	20 kg × 2
				(0·32*L*, −5°)	(0·33*L*, 185°)	1 kg × 4
				(0·38*L*, −5°)	(0·38*L*, 185°)	
1·6	−55·60	−62·47	0	(0·35*L*, −5°)	(0·35*L*, 185°)	10 kg × 2
				(0·32*L*, −5°)	(0·32*L*, 185°)	1 kg × 4
				(0·38*L*, −5°)	(0·38*L*, 185°)	
1·7	−56·77	−62·45	90	(0·35*L*, −5°)	(0·35*L*, 185°)	10 kg × 2
				(0·32*L*, −5°)	(0·32*L*, 185°)	1 kg × 4
				(0·38*L*, −5°)	(0·38*L*, 185°)	

forces are applied symmetrically to the shell, the addition of only one absorber breaks the symmetry of the system. In the absence of symmetry, the dominant acoustic modes (3, 1, 1) and (4, 1, 1) are excited and result in a significant increase in the acoustic *PE*. In order to retain the symmetry property, a second absorber is attached to the shell at the force location (0·35*L*, 185°) (case 1.2) and the mass of each absorber is chosen to be 20 kg. A substantial reduction of both energies to 62 dB is now observed since the point forces provided by the absorbers almost cancel out the external point forces. In this case, the reduction in the *KE* of the shell is exactly equal to the reduction in the acoustic *PE*. This equivalence is based on the fact that the external forces and the absorber-forces are of the same type and are at the same locations. If another two absorbers, located at (0·35*L*, 90°) and (0·35*L*, 270°) and with a mass of 10 kg each, are used together with the previous two absorbers (case 1.3), only a small improvement in reducing the acoustic *PE* is obtained. From the numerical data, these two extra absorbers are seen to exert very small forces on the shell. They are also located at the nodes of the $m_2 = 1$ vibrating modes and consequently have little effect on the vibration and the sound field. Therefore, the most important absorbers for reducing the vibration and the noise are those placed at the locations at which the external point forces apply. These absorbers are referred to as central absorbers in this paper.

Although the arrangement of absorbers in case 1.2 gives impressive results, some attempt still needs to be made to gain an understanding of the effects of changing the mass of the absorbers. First, two additional dynamic absorbers, each with mass 10 kg, called auxiliary absorbers, are attached to the shell near each central absorber (case 1.4). A similar reduction in the *KE* of the shell, as in case 1.2, is achieved. Surprisingly, the reduction in the *PE* of the sound field, as observed from the numerical result, is much larger; even though the resultant forces caused by the auxiliary absorbers are found to be much smaller than the central ones. This phenomenon suggests that the reduction may be insensitive to the mass of auxiliary absorbers. To examine this hypothesis, the mass of each auxiliary absorber is then reduced to 1 kg (case 1.5), which is much smaller than that of the central

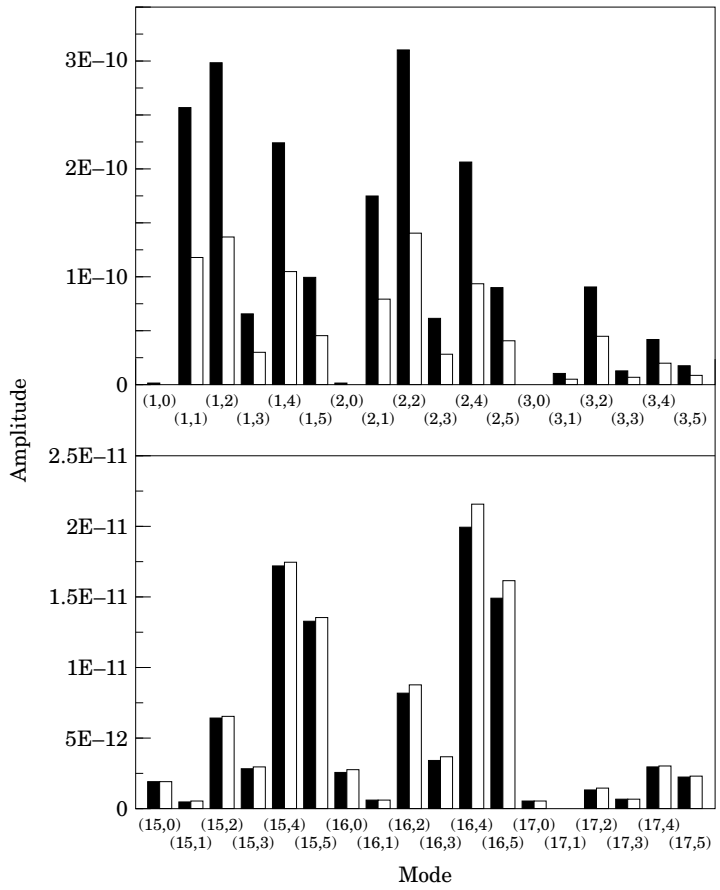

Figure 5. Amplitudes of vibrating modes due to external point forces: (a) $m_1 = 1, 2, 3$, (b) $m_1 = 15, 16, 17$; ■, case 1.2; □, case 1.5.

absorber and the result shows only a very small difference from the previous case. Figure 5 presents the total amplitude, defined as $\Sigma_{m_3=1}^{2}[u_{m_1m_2m_3}u^*_{m_1m_2m_3}]^{1/2}$, of the (m_1, m_2) symmetric and asymmetric vibrating modes for case 1.2 (without auxiliary absorbers) and case 1.5 (with 8 auxiliary absorbers) when the amplitude of each external force is 20 N. The presence of the light auxiliary absorbers is seen to increase the stiffness of the shell around the center locations. This suppresses the vibration of modes with small m_1 values and enhances the higher vibration modes with large m_1 which are not well coupled with the sound field. Therefore, the *KE* of the shell remains nearly the same while the acoustic *PE* level decreases substantially. The data from case 1.6 in Table 2 is for the same arrangement of absorbers but using lighter central absorbers, and the results are observed to be inferior to the results obtained in the previous case. In conclusion, the mass of the central absorbers is found to dominate in the reduction of the *KE* while the additional auxiliary absorbers, even with small masses, may produce a further attenuation in *PE*.

Figure 6(a) illustrates the effects of changing the masses of the absorbers in case 1.6. The abscissa of this figure is the mass of the central absorber. Here, the mass of each auxiliary absorber is always kept at 1/10 of the mass of the central absorber. As expected,

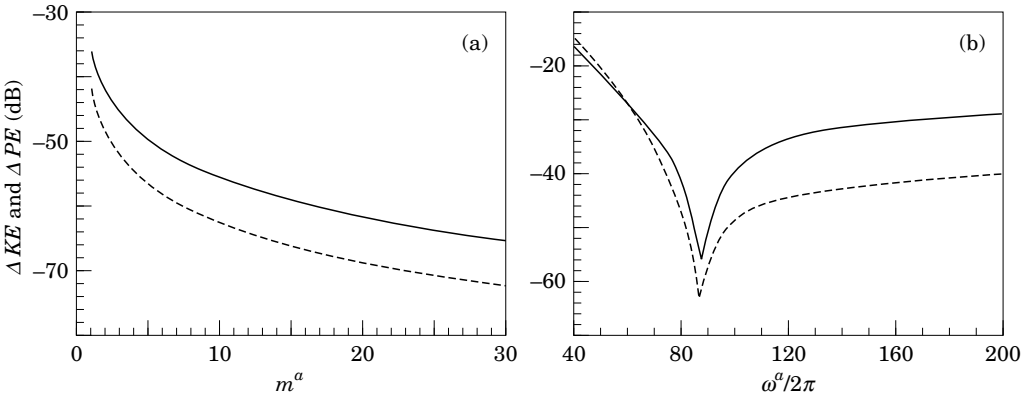

Figure 6. Reduction in *KE* and *PE* for external point forces as function of (a) mass of absorber, (b) frequency of absorber: ——, reduction in *KE*; – – –, reduction in *PE*.

a greater reduction of *KE* and *PE* is obtained when the masses of absorbers are increased. The resultant effects due to varying the natural frequency of the absorbers are given in Figure 6(b). Not surprisingly, the optimum reduction in vibration and acoustic energies occurs when the natural frequency of absorbers is exactly equal to the excitation frequency.

The above discussions are also valid for other center locations and for other phase difference values between two forces as long as the external excitations are point forces. The numerical results for $\theta_p = 90^\circ$ are given in case 1.7 of Table 2. The same absorber-placement as case 1.6 is used and it yields results close to those in case 1.6. It is worth mentioning that, before adding the absorbers, the *KE* of the shell and the acoustic *PE* for $\theta_p = 90^\circ$ are about 1·6 dB and 17·8 dB larger than those for $\theta_p = 0^\circ$. This significant difference in *PE* attributed to the observation that the two external forces with $\theta_p = 90^\circ$ create large, asymmetric $m_2 = 1$ vibrating modes. These modes, as discussed previously, have the largest energy efficiencies and can therefore affect the sound field to the greatest extent. This result, due to the changing synchrophase angle, is similar to what has been observed previously [4].

5.3. RESULTS DUE TO UNIFORMLY DISTRIBUTED PRESSURES

Consider two uniformly distributed pressures applied to the shell. The central locations of the forces, $(\bar{x}, \bar{\theta}) = (0{\cdot}35L, -5^\circ)$ and $(0{\cdot}35L, 185^\circ)$, are the same as the point forces described previously and the phase difference θ_p between the two distributed forces is defined as in the previous section. Suppose the two sides of each distribution area are 1 m in the x direction and 0·25 m in the θ direction. The vibration and the sound reduction effects obtained by adding absorbers are shown in Table 3. The dominant modes of vibration for $\theta_p = 0^\circ$ are found to be the $m_2 = 1$ modes with antinodes at 90° and the $m_2 = 2$ modes with antinodes at 0°. For the first case, two absorbers, each with a mass of 20 kg, are placed at $(0{\cdot}35L, 90^\circ)$ and $(0{\cdot}35L, 270^\circ)$ (case 2.1) so as to eliminate the $m_2 = 1$ modes which have large energy efficiencies. After introducing the absorbers, the $m_2 = 1$ modes are slightly decreased; however, the modes corresponding to the larger m_2 values are increased. Thus, the *KE* of the shell and the acoustic *PE* are found to remain almost the same. In case 2.2, more absorbers being added near the locations of the above-mentioned absorbers still cannot change the results significantly. The authors' efforts are now turned to cancelling the external forces directly via absorbers at the center

TABLE 3

Reduction in KE and PE for external, uniformly distributed forces

Case	Δ *KE* (dB)	Δ *PE* (dB)	θ_p(°)	area	locations of absorbers	m^a
2·1	+0·008	−0·40	0	1·0 × 0·25	(0·35*L*, 90°) (0·35*L*, 270°)	20 kg × 2
				(0·35*L*, 90°)	(0·35*L*, 270°)	20 kg × 2
2·2	+0·007	+0·06	0	1·0 × 0·25	(0·32*L*, 90°) (0·32*L*, 270°)	1 kg × 4
				(0·38*L*, 90°)	(0·38*L*, 270°)	
2·3	−5·92	−5·24	0	1·0 × 0·25	(0·35*L*, −50°) (0·35*L*, 185°)	20 kg × 2
2·4	−9·30	−9·62	0	1·0 × 0·25	(0·35*L*, −5°) (0·35*L*, 185°)	20 kg × 2
				(0·32*L*, −5°)	(0·32*L*, 185°)	1 kg × 4
				(0·38*L*, −5°)	(0·38*L*, 185°)	
2·5	−21·57	−23·14	0	1·0 × 0·25	(0·35*L*, −5°) (0·35*L*, 185°)	20 kg × 2
				(0·32*L*, −5°)	(0·32*L*, 185°)	1 kg × 8
				(0·38*L*, −5°)	(0·38*L*, 185°)	
				(0·35*L*, −10°)	(0·35*L*, 0°)	
				(0·35*L*, 180°)	(0·35*L*, 190°)	
2·6	−21·55	−23·05	0	1·0 × 0·25	(0·35*L*, −5°) (0·35*L*, 185°)	1 kg × 10
				(0·32*L*, −5°)	(0·32*L*, 185°)	
				(0·38*L*, −5°)	(0·38*L*, 185°)	
				(0·35*L*, −10°)	(0·35*L*, 0°)	
				(0·35*L*, 180°)	(0·35*L*, 190°)	
2·7	−0·61	−2·41	0	4·0 × 0·5	(0·35*L*, −5°) (0·35*L*, 185°)	1 kg × 10
				(0·32*L*, −5°)	(0·32*L*, 185°)	
				(0·38*L*, −5°)	(0·38*L*, 185°)	
				(0·35*L*, −10°)	(0·35*L*, 0°)	
				(0·35*L*, 180°)	(0·35*L*, 190°)	
2·8	−23·13	−23·90	90	1·0 × 0·25	(0·35*L*, −5°) (0·35*L*, 185°)	1 kg × 10
				(0·32*L*, −5°)	(0·32*L*, 185°)	
				(0·38*L*, −5°)	(0·38*L*, 185°)	
				(0·35*L*, −10°)	(0·35*L*, 0°)	
				(0·35*L*, 180°)	(0·35*L*, 190°)	

locations. If two central absorbers (case 2.3), each with a mass of 20 kg, are used, then a reduction of approximately 5 dB in both *KE* and *PE* is obtained. The results are improved much more than those in case 2.2; nevertheless, they are still unsatisfactory compared to those in the preceding section for external point forces. This suggests that the effects of distributed forces cannot be completely cancelled out through the use of a few absorbers which apply only point forces to the structure. To overcome this problem, two auxiliary absorbers (5 kg each) are added near each central absorber (case 2.4). The reduction in *KE* and *PE* now becomes superior to case 2.3. The performance can be further improved by the use of additional auxiliary absorbers. The data in case 2.5 of Table 3 are obtained using four 1 kg auxiliary absorbers around each central absorber. This arrangement yields a reduction in the *KE* of the shell and the acoustic *PE* of approximately 22 dB. In fact, one may suspect that there is no need for heavy central absorbers since the external forces are distributed forces rather than concentrated forces. Moreover, the magnitudes of masses of the absorbers are found to have only a small influence on the reduction results. Numerical investigation reveals that the mass of each absorber can be

described to 1 kg (case 2.6) and similar results of 21·5 dB reduction in *KE* and 23·1 dB in *PE* are still achieved.

More data are given in Figure 7(a) in which the reduction in *KE* and *PE* for varying masses of absorbers is presented. The curves represent the results obtained when the same arrangement of absorbers as in case 2.6, and every absorber has the same mass. The reduction effects seem to become saturated, i.e., the resultant *KE* and *PE* remain almost constant, when the mass of an individual absorber exceeds 2·5 kg. This is a distinctly different behavior from the use of absorbers on simple dynamic systems or on structures excited by only external point forces. The results suggest that light, distributed dynamic absorbers, near the distributed pressure locations, may be the best choice for reducing the vibration of a structure and the accompanying acoustic pressure generated by external uniformly distributed forces. The effects of changing the natural frequencies of absorbers are given in Figure 7(b) for the same absorber-placement. Unlike the conclusions drawn for the shells subject to external point forces presented in the previous section, the maximum reduction in the *KE* of the shell and the acoustic *PE* does not happen in the tuned case. The largest decrease in the acoustic *PE* is found when the frequencies of the absorbers are slightly larger than the excitation frequency. The greatest reduction in the *KE* of the shell vibration occurs at an even higher excitation frequency. Similar conclusion was also presented by Fuller *et al*. [9]. This result suggests that detuned dynamic absorbers may do a better job of reducing the vibration and the noise from external disturbances of the distributed types. The use of detuned absorbers for reduction in the vibration of continuous structures and in the accompanying noise is conceptually different from using tuned absorbers in vibrating systems with one or two degrees of freedom.

If the area of the distributed pressure is extended to 4 m × 1 m, i.e., the external forces are more spread out, worse results are obtained for the same absorber-arrangement (case 2.7). This phenomenon is expected since this external excitation is far from a point force, and more vibration modes participate in the response compared to case 2.6. Adding more absorbers over broader areas near the distributed pressures is suggested to obtain better reduction effects.

Even though the complete data are not shown here, similar results and conclusions are obtained for different center locations and for other values of θ_p. The results for two external forces with $\theta_p = 90^\circ$ are given in Table 3. The reduction in *KE* and *PE* improves a small amount compared to that of case 2.6 when $\theta_p = 0^\circ$. Note that, after adding

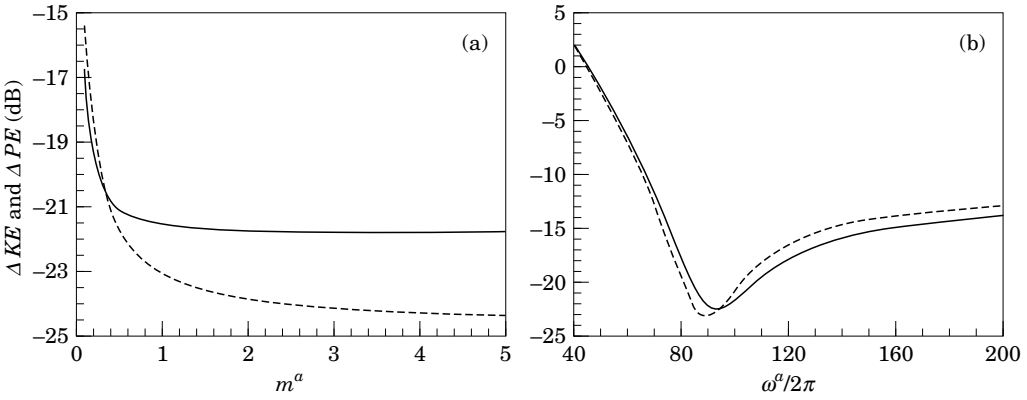

Figure 7. Reduction in *KE* and *PE* for external uniformly distributed forces as function of (a) mass of absorber, (b) frequency of absorber: ——, reduction in *KE*; – – –, reduction in *PE*.

absorbers, the resultant KE and PE for $\theta_p = 90^\circ$ are still much larger compared to their values when $\theta_p = 0^\circ$ although the reduction for the former case seems slightly better.

6. CONCLUSIONS

The dynamic behavior of a closed cylindrical shell, representing an aircraft fuselage with added dynamic absorbers, has been analyzed. The interior sound field of the shell was also investigated. The vibration and the sound level of the enclosed acoustic field are successfully reduced by adding dynamic absorbers at appropriate positions. The reduction of the kinetic energy of the shell vibration and the potential energy of the sound pressure were studied. The results were discussed for two different types of external forces—point forces and uniformly distributed pressures. In addition, the effects of varying the parameters of the absorbers were investigated and accordingly some design guidelines were suggested.

For cylindrical shells subject to external point forces, placing a heavy central absorber at each force location and several light absorbers near to it can result in the best reduction of vibration and of noise. Perfectly tuned absorbers, in this case, give the greatest reduction in the kinetic energy of the shell and the acoustic potential energy. In addition, the use of heavier center absorbers generally yields greater reductions. On the other hand, for uniformly distributed excitations, several light-weight absorbers scattered on the area of each distributed pressure are proposed for the reduction of the shell vibration and the resultant interior sound. The best result is obtained when the common natural frequency of the absorbers is slightly detuned. Moreover, light absorbers are sufficient for effective reduction and the mass of absorbers does not affect the results as long as it exceeds a certain critical value.

REFERENCES

1. J. F. Wilby 1983 *SAE Paper* 830737. The prediction of interior noise of propeller-drive aircraft: a review.
2. C. R. Fuller and F. J. Fahy 1982 *Journal of Sound and Vibration* **81**, 501–518. Characteristics of wave propagation and energy distribution in cylindrical elastic shell.
3. C. R. Fuller 1984 *Journal of Sound and Vibration* **96**, 101–110. Monopole excitation of vibrations in an infinite cylindrical elastic shell filled with fluid.
4. C. R. Fuller 1986 *Journal of Sound and Vibration* **109**, 141–156. Analytical model for investigation of interior nosie characteristics in aircraft with multiple propellers including synchrophasing.
5. D. R. Thomas, P. A. Nelson and S. J. Elliott 1993 *Journal of Sound and Vibration* **167**, 91–111. Active control of the transmission of sound through a thin cylindrical shell, Part I: the minimization of vibration energy.
6. D. R. Thomas, P. A. Nelson and S. J. Elliott 1993 *Journal of Sound and Vibration* **167**, 112–128. Active control of the transmission of sound through a thin cylindrical shell, Part II: the minimization of acoustic potential energy.
7. A. Berry and J. Nicolas 1994 *Applied Acoustics* **43**, 185–215. Structural acoustics and vibration behavior of complex panels.
8. C. R. Fuller 1985 *AIAA Paper* 85–0879. Mechanisms of transmission and control of low-frequency sound in aircraft interior.
9. C. R. Fuller, J. P. Maillard, A. H. von Flotow and M. Mercadal 1995 *Proceedings of First Joint CEAS/AIAA Aeroacoustics Conference*, Germany. Control of aircraft interior noise using globally mis-tuned vibration absorbers.
10. J. D. Jones and C. R. Fuller 1983 *Proceedings of the 6th IMAC Conference*, Florida, U.S.A. Reduction of interior sound fields in flexible cylinders by active vibration control.
11. B. J. Brevart and C. R. Fuller 1993 *Journal of Acoustical Society of America* **94**, 1467–1475. Active control of coupled wave propagation in fluid-filled elastic cylindrical shells.

12. D. S. Mandic and J. D. Jones 1989 *AIAA Paper* 89–1075. Adaptive active control of enclosed sound fields in elastic cylinders via vibrational inputs.
13. M. A. Simpson, T. M. Luong, C. R. Fuller and J. D. Jones 1991 *Journal of Aircraft* **28**, 208–215. Full-scale demonstration tests of cabin noise reduction using active vibration control.
14. G. P. Mathur and B. N. Tran 1993 *AIAA Paper* 93-4437. Aircraft cabin noise reduction tests using active structural acoustic control.
15. P. A. Nelson and S. J. Elliott 1992 *Active Control of Sound*. London: Academic Press.
16. A. J. Bullmore, P. A. Nelson and S. J. Elliott 1990 *Journal of Sound and Vibration* **140**, 191–271. Theoretical studies of the active control of propeller-induced cabin noise.
17. C. R. Fuller and J. D. Jones 1987 *Journal of Sound and Vibration* **112**, 389–395. Experiments on reduction of propeller induced interior noise by active control of cylinder vibration.
18. D. J. Inman 1994 *Engineering Vibration*. NJ, Prentice-Hall.
19. A. H. von Flotow, A. Beard and D. Bailey 1994 *Proceedings of Noise Conference* 94, Florida, U.S.A., 389–394. Adaptive tuned vibration absorbers: tuned laws, tracking agility, sizing, and physical implementations.
20. E. H. Waterman, D. Kaptein and S. L. Sarin 1983 *SAE Paper* 830736. Fokker's activities in cabin noise control for propeller aircraft.
21. W. G. Halvorsen and U. Emborg 1989 *SAE Paper* 891080. Interior noise control of the SAAB 340 aircraft.
22. A. W. Leissa 1973 *Vibration of Shells*, Washington, D.C.: NASA.
23. F. Fahy 1985 *Sound and Structural Vibration*: *Radiation*, *Transmission and Response*. London: Academic Press.
24. S. Temkin 1981 *Elements of Acoustics*. New York: John Wiley.